CHARACTERIZATION OF EXOSOMES FROM GLIOMA CELLS UNDER HYPOXIA AND OXIDATIVE STRESS

KATARINA TOMAZIN

Master´s Degree Project
January, 2015

Faculty of science
Department of biology
Molecular biology, specialization in Medical biology

Characterization of exosomes from glioma cells under hypoxia and oxidative stress

Katarina Tomazin

Exosomes are cell-secreted nanosized (30-200 nm) membrane vesicles that contain cytosol proteins and nucleic acids (mRNA, miRNA and mDNA). They have been characterized to be released by most cell types and thus, represent an important part of cell-cell communication. Especially they might play an important role in cell adaptation processes to stress conditions such as hypoxia or oxidative stress. The main difficulty in studying exosomes is however their purification and characterization process which is still a major challenge in the field of exosome research. In this study, we set up the method for isolation of exosomes with differential centrifugation and two characterization techniques nanoparticle tracking analysis (NTA) and bicinchoninic acid assay (BCA). With the latter techniques we studied whether glioma cells exposed to stress conditions produce more exosomes as communication messengers compared to standard environment. The study so far did not answer this question, our data nevertheless show the initial evidence that exosomes reflect the inner metabolic status of cells.

Introduction

Exosomes and their importance

Cells are basic structural units of all living organisms. In order to form functional multicellular living systems, communication is vital. Traditionally it was believed that this intercellular communication depended only on physical contact between cell membranes and by free diffusion of small cell-secreted soluble molecules such as neurotransmitters, hormones and cytokine (1). In the past three decades, it has been revealed that, in addition, a big portion of the cell-cell communication is relayed by membrane vesicle trafficking (2, 3). The discovery of molecular mechanisms that drive the delivery of membrane vesicles and their cargo to the right target at the right time was recently awarded by the 2013 Nobel Prize in Physiology or Medicine, highlighting the importance of this cell process (4). These cell-secreted lipid vesicles can be categorized into three types, depending on how they are formed. Apoptotic bodies are released during apoptosis, process of programmed cell death, varying in size from 500 -2000 nm, whereas microvesicles and exosomes are extracellular vesicles released form healthy cells. The former are produced by outward budding of the cell membrane which releases vesicles with a size varying from 50 -1000 nm (3). These have been observed to be largely involved in, for example, tumor progression and inflammation (5, 6). Exosomes, studied in this paper, are instead formed inside the cells as a part of the endosomal pathway. Briefly, primary endocytic vesicles are generated by endocytosis and are later fused with the plasma membrane into an early endosome that matures to a late endosome or a so-called multivesicular body (MVB). Exosomes get loaded during that process with various types of proteins (e.g. derived from the Golgi complex (GC), endoplasmatic reticulum (ER), cytoplasm and lipid rafts) and genetic material from cytoplasm. Eventually the MVB fuses with the plasma membrane, resulting in the secretion of exosomes to the extracellular space (Figure 1) (7, 8). Due to their biogenesis, exosomes are generally considered to be smaller than other microvesicles with size varying between 30-200 nm in diameter (3, 9, 10). The estimate of exosome size range differs from one report to another since the different isolation

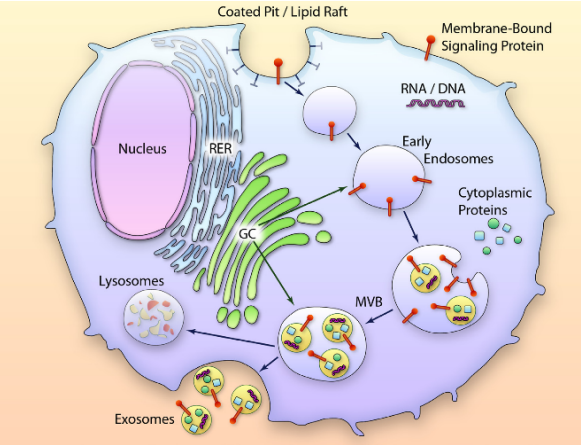

Figure 1: Biogenesis of exosomes. Exosomes are generated in the MVBs, late endosomal compartments, in the endosomal pathway inside the cell. They can carry various types of proteins derived from the GC, ER (in this case rough ER, RER), cytoplasm and lipid rafts that are directly sorted in the MVBs together with the mRNA, microRNA and mDNA from the cytoplasm. Exosomes are released to the extracellular space with the fusion of MVBs with the plasma membrane, or so-called exocytosis (10).

and characterization techniques may result in different size distributions as described below.

Cell-released vesicles were described for the first time in 1983 by Pan *et al.* where they were observed to be secreted by the reticulocytes into the extracellular space, carrying transferrine receptor on their surface (2). Four years later these vesicles were termed 'exosomes' and were characterized as particles that discarded unnecessary proteins from the reticulocytes during their maturation (11). For many years they were thought to be a cellular disposing machinery of cell debris and unneeded membrane proteins (12). Subsequent research led to the discovery that exosomes were involved in much more complex functions, such as antigen presentation, immune suppression and tumor invasiveness (8, 12, 13). These discoveries have led to an increased interest in the exosome research field that drastically expanded since then (12).

The structure of the exosome was shown to consist of a lipid bilayer membrane with the presence of membrane proteins (8). This membrane is encapsulating an aqueous core of soluble proteins and genetic material (8, 14). The composition of their cargo may differ depending on the cell of origin but generally exosomes carry in their membranes specific subclasses of proteins, reflecting their intracellular site of origin, which can be used as exosomal markers (8, 15). These specific subclasses include mainly tetraspanins (e.g. CD9, CD63 and CD81), but also cytoplasmic proteins (e.g. actin, annexins, Rab proteins) and heat shock proteins (e.g. Hsc70, Hsp90) (8, 12). Genetic material inside the exosomal core is composed of messenger RNA (mRNA), small non-coding micro RNA (miRNA) and mitochondrial DNA (mtDNA) that can be transported to recipient cells (Figure 2) (14, 16). When transferred to a recipient cell, exosomal mRNA can be translated into proteins (14) and miRNA can modulate the gene expression (17).

Packaging of exosomal content inside the cell was shown not to be random but rather selective. Several reports have demonstrated that specific mRNAs, miRNAs and proteins are enriched in exosomes of the donor cell through yet unknown selective mechanisms (9, 14). The selective packaging can thus depend on different conditions the donor cell is in (e.g. natural, hypoxia, oxidative stress) or on the differential availability of material in the cell due to changed extracellular conditions (18, 19). Following secretion of exosomes to the extracellular space, they can interact with other cells and induce various physiological changes (12). These mechanisms of interactions have not been completely understood but studies suggested that exosomes can interact with the recipient cells in multiple ways. Fusion of the lipid bilayer-surrounded exosome with the recipient plasma cell membrane results in the release of the exosomal content into the recipient cell (9). Other proposed mechanisms are that exosomes can bind to a specific receptor expressed on the target cell which facilitates the uptake (20) or endocytosis followed by the fusion of exosomes into the endosomal pathway (21).

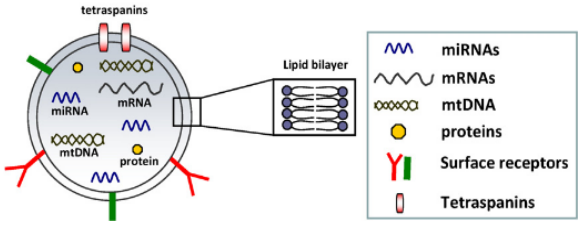

Figure 2: Exosome composition. Exosomes consist of a lipid-bilayer that encapsulates a core of proteins and genetic material (miRNA, mRNA, mtDNA). On the membranes they display different types of proteins such as tetraspanins, cytoplasmic proteins, heat-shock protein and surface receptors. Tetraspanins are most commonly used as exosomal markers, for example CD63 and CD81 (12).

Since the exosomes were first discovered, several studies have demonstrated that a wide range of cell types have the ability to generate exosomes, including tumor cells, dendritic cells, B cells, T cells, epithelial cells, mast cells, platelets, cells in neuron system and stem cells (12, 14, 15, 22). Moreover, most cells in the nervous system, such as neural stem/progenitor cells, neurons, astrocytes, microglia, and oligodendrocytes, have the capability to release exosomes (23-26). Exosomes, released from different cell types, can cause a variety of physiological and pathological changes to the recipient cell, depending on the cell of origin and the secretion conditions (12, 15). For example, mast cells can secrete exosomes that promote activation of B and T lymphocytes and hence trigger immune responses (27). It is also well studied that various types of tumor cells (e.g. breast, brain and lung) produce high amounts of exosomes, correlating with the stage of malignancy. These have the ability to manipulate the tumor microenvironment therefore promoting tumor growth and invasion (15). For example, glioblastoma-derived exosomes were shown to activate angiogenic response by endothelial cells (9). What is more, due to the stability of the exosomes, they can travel to distant parts of the body through body fluids and possibly alter the endothelium, contributing to the larger metastatic potential of a tumor (28).

Exosomes have been found to be present in body fluids, including human plasma, serum, urine, breast milk and bronchoalveolar fluid of healthy individuals (29). In some diseases (e.g. cancer) can their amounts in serum drastically increase and exosomes might therefore be used as diagnostic markers since they can display the tumor characteristics in surface molecules and carry tumor-associated mRNAs and miRNAs (12). Furthermore, due to the ability of most cells to uptake exosomes there has been research aiming towards their use as delivery vehicles for therapeutic applications (30). One advantage of this approach is that the exosomes compared to other delivery vesicles are very stable in body fluids but also less immunogenic if the patient's own cells are used for their production (31).

Methodological considerations

The process of isolating and characterizing exosomes is still a debated topic and a major challenge in the field of exosome research since they are mixed with the other membrane vesicles in the extracellular environment. Generally exosomes are collected from the body fluids or from the supernatant of cultured cells grown in the defined medium or medium with fetal bovine serum that has prior been depleted of exosomes (32). These samples need to be later purified by multiple centrifugation steps. First of all, low *g*-force centrifugation (500 – 1000 x *g*) is used to remove the cells and bulky cell debris followed by higher *g*-force centrifugation (16000 – 20000 x *g*) to remove apoptotic bodies and microvesicles (14, 32, 33). Finally, the exosomes containing pellet is obtained by ultracentrifugation at a very high *g*-force (100000 – 120000 x *g*) (14). The major drawback of differential ultracentrifugation protocols is that co-sedimentation can occur due to overlapping density of protein aggregates or large microvesicles together with exosomes, which makes the sample less pure (33, 34). This can to some degree be overcome by applying an additional washing step with PBS after exosomes are already isolated (32). Some protocols use a 0.22 µm

filtration step before the ultracentrifugation to further remove apoptotic bodies and larger microvesicles (14). However, that technique is also used for the preparation of liposomes by extrusion. In fact bigger lipid particles pushed through a filtration membrane can break into smaller particles, hence resulting in the opposite result that was initially intended (35). Therefore the use of this type of filtration in exosomes isolation is undesirable. Additionally, protein aggregates and larger microvesicles can be separated from exosomes by ultracentrifugation using a linear sucrose gradient where the difference in flotation velocity is used to divide these particles according to buoyant density. Most studies report that exosomes have a flotation density of 1.08-1.22 g/ml (28, 33).

Various qualitative and quantitative methods can be used in a complementary fashion in order to characterize the exosome-containing pellet and assess its purity. Total particle concentration can be measured by nanoparticle tracking analysis (NTA), which is based on the Brownian motion of particles in solution. All particles in a fluid have a movement that is determined by their size and the temperature. In NTA, a laser beam illuminates the particles which generate a scatter signal that is sensed by a detector. These scattering particles are then individually tracked in a time-lapse video by the NTA software which calculates vesicle size and total concentration depending on their diffusion properties (36). Another way of estimating the exosome concentration is based on the total protein content of exosomes. The protein content can be quantified using the bicinchoninic acid (BCA) colorimetric assay (37, 38). The assay spectrophotometrically measures the light absorption of a complex that is formed between the assay reagent and the proteins in the sample. The protein concentration is then calculated by plotting the signal from the sample against the standard curve obtained using bovine serum albumin (BSA) protein standards (38). The protein extracts can be further used to quantify the presence of exosomal markers (most often CD63 or CD81) or contaminants (endoplasmic reticulum or Golgi apparatus markers) (14, 39, 40). Such quantification is most commonly performed by Western blot which is an analytical technique that can detect specific proteins in a sample. Briefly, proteins are first separated by size with gel electrophoresis and then transferred onto a membrane where they are stained with the specific antibodies targeting proteins of interest. (41). The full exosomal proteome can be characterized with high-throughput proteomic techniques, as for example with mass spectrometry (MS). MS is an analytical technique used for identification and quantification (under specific experimental configurations) of proteins in a sample. Firstly, proteins are proteolytically cleaved with a digestive enzyme (most often trypsin) into smaller peptides. These are then ionized and some selected ions are further fragmented, which result in mass over charge spectra. Data analysis allows comparing the obtained mass over charge ratios of the fragments against those of known sequences in a database. Taking into account also the intensities of the spectral features and the theoretical sequence and spectra of protein fragments, the peptides with best matching spectra are identified and assigned to the most probable protein they constitute (42).

Gliomas and angiogenesis

Glioma is a type of cancer that arises from glial cells that have gone through neoplastic transformation to turn into malignant tumor cells. There exist several types of glial cells (e.g. astrocytes, oligodendrocytes) and glioma can therefore form different types of tumors according to the originating glial cell type (43). For example, astrocytoma is a type of glioma that arises from astrocytes, the most abundant type of glial cells in the brain (43, 44). The World Health Organization (WHO) classifies malignant gliomas into the three stages II-IV according to their development stage which in turn correlates strongly with patient survival rate. Stages II and III are considered as low-grade gliomas, while the IV stage is highly malignant

glioma that is characterized by the poorest survival rate of patients (45). To elucidate the role of exosomes in brain cells, the two human-derived glioma cell lines, U87-MG and H4 were used. U87-MG cell line is a long established and well-studied grade IV glioma, also referred to as glioblastoma multiforme, the most malignant form of astrocytoma (46). H4 cell line was instead derived from a patient with neuroglioma, (low-grade astrocytoma) (47).

Progression from low-grade malignancy to high-grade malignancy is in large driven by the increase in proliferative capacity of tumor cells and angiogenic events (i.e. formation of new blood vessels from the pre-existing vasculature) in the hypoxic regions of the tumor (43, 48). Hypoxic regions are parts in the body that are low in oxygen and nutrients supply from the blood vessels which is a necessary requirement for a cell to properly function. The cells in the body are normally positioned in a close proximity at most 100 μm away from the blood vessels where the diffusion of oxygen and nutrients from the vessels is still possible (48). Since the tumor cells rapidly proliferate, they can outgrow their blood supply which can in turn cause vascular endothelial injury resulting in a significantly lower oxygen levels or so called hypoxic regions (43, 45). Due to cellular need for delivery of nutrients from the blood, cells in those regions start dying which result in the tumor necrotic centers. Cells surrounding the glioma necrotic centers, are called pseudopalisading cells. They can start to secrete hypoxia-related angiogenic factors, such as vascular endothelial growth factor (VEGF), that stimulate microvascular proliferation and create new source of blood supply (43, 45, 48). Consequently, the tumor may become even more progressive and possibly enriched in apoptosis-resistant clones that are able to survive hypoxic microenvironments (43). Necrosis and highly increased angiogenesis are the main histopathologic features of glioblastoma that distinguish it from the low-grade astrocytomas (48).

The intracellular events that induce tumor angiogenesis are highly connected to hypoxic microenvironment and are driven by hypoxia inducible factor 1 α (HIF-1α) and its downstream targets (49). HIF-1α is a constitutively expressed protein that is differentially altered under normoxia compared to hypoxia. In normoxia HIF-1α is hydroxylated at prolyl residues by hydroxylase enzymes. That allows the von-Hippel-Lindau protein (pVHL) to ubiquitinate HIF-1α , leading to proteasomal degradation (50). In hypoxia however, these hydroxylases are inactivated because they require oxygen for catalysis of the hydroxylation reaction (48). Therefore, HIF-1α protein remains stable in hypoxic condition and can translocate to the nucleus where it dimerizes with the HIF-1β subunit. The dimer can then bind to hypoxia-responsive elements (HREs) which can activate the promoters of genes that are involved in various processes, such as angiogenesis, cell proliferation, survival, extracellular matrix metabolism and others (48). Among major angiogenesis driving factors that have been found upregulated in hypoxic cells are VEGF, VEGF receptors (VEGFR), angiopoietin and matrix metalloproteinases (MMPs) (51). VEGF is a growth factor that is abundantly expressed by hypoxic cells (in glioblastoma especially by pseudopalisades) and is released into the extracellular matrix (45, 52). The formation of gradients for VEGF and other proangiogenic factors in the microenvironment promotes the proliferation of endothelial cells as well as the formation of new vasculature (52).

Hypoxic and oxidative stress

According to previous studies, hypoxia is considered a major regulator of tumor development and aggressiveness but the underlying mechanisms of how the cells adapt or communicate with their surrounding microenvironment are still remaining questions (39, 49, 51). Cell-secreted nanovesicles, exosomes, may play an important role in that communication (28, 39). Recent reports have shown that the

exosomes from hypoxic cells were excreted in higher amounts and were enriched in hypoxia-regulated mRNAs and proteins reflecting hypoxic status of donor cells (18, 39, 53). Furthermore, hypoxic exosomes have been shown to mediate an angiogenic response by endothelial cells *in vitro* (28, 39).

In vitro the hypoxia response can be activated either physically or chemically. A hypoxia chamber can be used to create a controlled and isolated environment where the oxygen level can be reduced to reach near anoxia (0% O_2). Chemically induced hypoxic response is instead reached using compounds that interrupt the HIF-1α pathway (54). For example, 2, 2'-dipyridyl (DIP) is an iron chelator that interrupts prolyl and asparaginyl hydroxylase enzymes (55, 56). Normally, hydroxylases require oxygen but also iron as a cofactor for their activity. When the iron pool in the cell is depleted as it is with iron chelators, the hydroxylases are inactive (57). Consequently, HIF-1α is stabilized and can translocate into the nucleus where it induces a hypoxia response (55-57).

Exosomes may also have an important role in cell communication in other types of stresses, such as oxidative stress (19). Reactive oxygen species (ROS), including hydrogen peroxide (H_20_2), are normal byproducts of cellular aerobic metabolism which can be neutralized by the cells innate cellular defense mechanisms (e.g. antioxidants, enzymatic scavengers) (19, 58). However, if the ROS levels increase to a point where the cell cannot eliminate them properly, ROS can cause serious damage to DNA, proteins and lipids which in turn can lead to a wide variety of diseases (58). Depending on the ROS concentration, the cellular response can range from proliferation, growth arrest and senescence to cell death. All these responses are activated by intracellular stress signaling pathways. However, it has also been reported that cells exposed to a low concentration of ROS can induce a tolerance to a higher dose of oxidative stress (59). Furthermore, a recent study showed that exosomes from donor cells exposed to oxidative stress carry protective signals to recipient cells and this way induce a tolerance resulting in reduced cell death (19).

Hypothesis

The main goal of this study was to establish a routine procedure for exosomes analysis including collection, isolation, quantitative and qualitative characterization. Since exosomes are known to be secreted under stress conditions and carrying signals important for a variety of cellular process (e.g. angiogenesis, stress resilience, tumor invasion, etc.) we set up a model of stress in glioma cell lines in order to study the differential release of exosomes. We hypothesized that U87-MG and H4 cells exposed to stress conditions would produce more exosomes than those in control environment. Moreover, we expect exosomes to carry stress-related information and we aimed to characterize their content in detail. The U87-MG cell line was used as a starting point to reproduce recent results (39) together with the H4 cell line. This initial set of experiments serves as a basis for further studies.

Materials and Methods

Cell culture

Human glioma cell lines (U87-MG and H4) were purchased from American Type Culture Collection (ATCC) and cultured in Dulbecco's modified Eagle medium (DMEM), supplemented with 10% dFBS (FBS with removed exosomes), 2 mM L-glutamin, 1 g/l glucose, 100 µg/ml streptomycin and 100 U/ml penicillin. All cells were cultured in a humidified incubator, set at 5% CO_2 and 37ºC.

MTT assay

Cells were plated in 96-well plates at a density of 4000 cells/cm^2 in a total volume of 100 µl of DMEM medium without phenol red, supplemented as described above. On

the day 1 after seeding, 25-100 µM concentration range of DIP and 10-400 µM concentration range of H_2O_2 were added into the wells. Since the DIP is dissolved in ethanol, that was added to the cells in the same concentrations as with DIP treatment and was used as control. The control for H_2O_2- treated cells was standard medium. Cells were then incubated for 48 hours and cell viability was measured with the 3-(4,5-Dimethylthiazol-2-yl)-2,5-Diphenyltetrazolium Bromide (MTT). MTT is reduced into insoluble formazan by cellular NADPH-dependent oxidoreductase enzymes. Those are active only in viable cells, thus the cell viability is measured according to the amount of produced formazan. Tetrazolium dye MTT in 5mg/ml concentration was added in 1:10 ratio to the wells and incubated in the cell culturing incubator for 3 h in dark. Formazan crystals were dissolved by adding 100 µl of acidified isopropanol that was prepared from 0.1 N HCl mixed in isopropanol. The plate was covered with aluminum foil and incubated at room temperature for 20 min. The optical density of formazan concentration was measured in a platereader at 570 nm. The signal at 690 nm was used to determine the background noise level and was subtracted. The absorbance values of formazan were used to plot dose-response curves for the two stress factors.

Cell counts with bright-field analysis

The experiment was designed in the same way as for the MTT assay, though black optical bottom plates were used. 48 hours after treatment cells were counted with the bright-field stain free analysis using the SpectraMax MiniMax 300 Imaging Cytometer.

Exosome isolation

U87-MG and H4 cells were cultured in DMEM supplemented with 10% dFBS to a high density. dFBS was obtained by ultracentrifugation using a Beckman centrifuge and rotor (70.1 Ti) at 120 000 *g* for 16h. Supernatant of FBS was filtered through 0.2 µm membrane filter prior to use in cells culture. The cells were cultured for 48 h in different conditions: control medium, 85 µM DIP (U87-MG), 60 µM DIP (H4) or 50 µM DIP (H4) and 70 µM H_2O_2 (U87-MG) or 25 µM H_2O_2 (H4). Exosomes were isolated by differential ultracentrifugation. At the end of the 48 h harvest time the conditioned media was collected for exosome isolation and the cells were trypsinized and counted with the use of a hemocytometer. Conditioned media were then centrifuged at 500 x *g* for 10 min to pellet the cells and cell debris. Supernatants were further centrifuged at 16500 x *g* at 4ºC for 20 min. Exosomes were in the end pelleted by ultracentrifugation at 120000 x *g*, 4ºC for 70 min. Exosomes were resuspended in 100 µl of PBS and frozen in -80ºC for further analyses.

Nanoparticle tracking analysis (NanoSight ™)

Isolated exosomes were diluted in PBS 100x and frozen in -80ºC till NTA analysis using NanoSight LM10 system, configured with a 405 nm laser and a high sensitivity digital camera system. Samples were injected in the prism chamber with a syringe and videos were collected and analyzed using the NTA-software. The same acquisition and analysis settings were used for different analysis. Each sample was measured three times.

Protein extraction and assay of protein concentration

Exosomes dissolved in PBS were broken down with the 3% SDS in RIPA buffer with protease inhibitors. RIPA buffer was prepared from 50 mM Tris-HCl, 137 mM NaCl, 1% Triton X-100, 0.1% SDS, one tablet of protease inhibitors (Roche) and miliQ water and the end pH was adjusted to 7,6-8. After adding 3% SDS in RIPA to exosomes, the Eppendorfs were vortexed and incubated on ice for 5 min. The protein content was then measured with Pierce® BCA protein Assay Kit by Thermo Scientific. The exosome lysates, plate blank (PBS), sample blank (3% SDS in RIPA buffer with PBS) and the BSA standards were pipetted into the wells of a 96-well half-bottom plate in amount of 12.5 µl. To

the wells was then added 100 µl of working reagent and the plate was slightly shaken and incubated for 30 min in 37 ºC. The plate was cooled to room temperature and the absorbance was measured at 562 nm in a plate reader (SpectraMax). The absorbance of the plate blank was subtracted from all the wells and the sample blank was substracted from the samples. The total protein concentration of exosomes was determined from the standard curve, plotted from 50-2000 µg/ml BSA standard concentration range.

Tandem mass spectrometry (MS/MS) using tandem mass tags (TMT)

Mass spectrometry based proteomics was performed by the Proteomic Core Facility at Sahlgrenska academy, Gothenburg University.

Sample preparation for proteomic analysis

100 µg of total protein of each sample and 100 µg of a pool containing equal amounts of all samples were diluted with lysis buffer to a volume of 70 µl. The samples were reduced by the addition of 2M DL-Dithiothreitol (DTT) to 100 mM and then trypsin digested using the filter-aided sample preparation (FASP) method modified from previously published protocol (60). After centrifugation the filtrates were subjected to isobaric mass tagging reagent TMT® according to the manufacturer's instructions (Thermo Scientific). Each sample was labelled with a unique tag from a TMT 6plex isobaric mass tag labeling kit, (http://www.piercenet.com/product/amine-reactive-6-plex-tandem-mass-tag-reagents). After TMT labeling, the samples in this set were pooled and concentrated. The peptides were further purified and fractionated into 12 fractions which were subsequently desalted.

LC-MS/MS Analysis

The dried fractionated and desalted 6-plexed TMT-labeled sample was reconstituted with 15 µl of 0.1 % formic acid (Sigma Aldrich)) in 3% acetonitrile and analyzed on an Orbitrap Fusion Tribrid mass spectrometer interfaced to an Easy-nLC II (Thermo Fisher Scientific). A second MS/MS analysis was performed excluding peptides already detected.

Database Search for protein TMT Quantification

All MS raw data files for the TMT set were merged for relative quantification and identification using Proteome Discoverer version 1.4 (Thermo Fisher Scientific). A database search was performed with the Mascot search engine (Matrix Science) using the human Swissprot Database version July 2014 (Swiss Institute of Bioinformatics, Switzerland). Only peptides unique for a given protein were considered for relative quantitation, excluding those common to other isoforms or proteins of the same family. The quantification was normalized using the protein median. The results were then exported to Excel for manual data interpretation, calculating fold changes and statistical analysis using Welch´s t-test in R.

Results

Modeling of stress conditions in glioma cell lines

Determination of suitable stress conditions for glioma cell lines U87-MG and H4 with two stress factors, DIP and H_20_2, was assessed with the MTT colorimetric assay and with the cell count using bright-field analysis by SpectraMax MiniMax 300 Imaging Cytometer. The dose-response curves to 25-1000 µM concentration range of DIP and 10-400 µM concentration range of H_20_2 are shown in Figure 3. Data points represent mean values of multiple individual experiments (as described below) that were performed at different time points using different concentration ranges of stress factors. Therefore, the calculated average value of each concentration was not always calculated from the same number of experiments. In the dose-response curve of U87-MG cell line, the data points represent four individual experiments with the exception of three and two concentrations

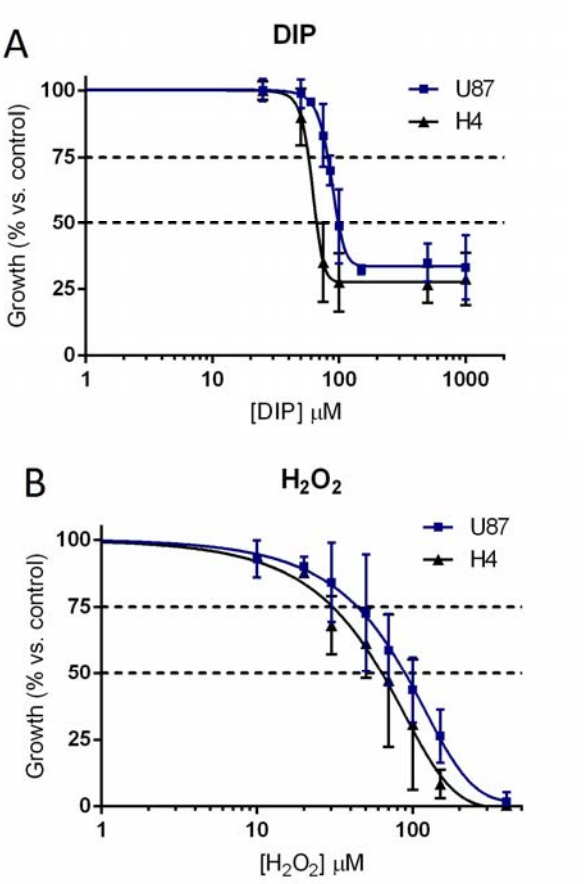

Figure 3: Dose-response curves from the MTT assay. Absorbance of formazan, measured on the 2nd day after the addition of stress factors in different concentrations, is representing amount of viable U87-MG and H4 cells. Absorbances of formazan from cells treated with different concentrations of stressors were compared to the control and the growth (y- axis) was calculated resulting in the dose-response curves of (A) DIP- treated (x-axis) and (B) H_20_2-treated (x-axis) cells. Fitted curves were plotted in GraphPad Prism 6.04 using log (inhibitor) *vs.* response nonlinear fit with variable slope. In all cases the bars denote ± standard deviation (SD) values. Dotted lines represent inhibitory concentrations IC25 and IC50 respectively which is presented in Table 1.

(for DIP and H_20_2 respectively) where mean values of two individual experiments were used. In the case of H4 cell line, the data points represent mean values of three individual experiments with the exception of two concentrations in H_20_2-treated cells where was used mean value of 1 individual experiment.

U87-MG cell line is more resistant to both types of stresses than H4 as shown by the shift to the right. Also, hydrogen peroxide induces its full inhibition of cell growth at

Table 1: Inhibitory concentration (IC) values from the MTT assay. IC25 and IC50 values were calculated from the dose-response curves of U87-MG and H4 cell lines (Figure 3) in GraphPad Prism 6.04 and they represent the concentrations (μM) of stress factors that inhibit cell growth by 25% and 50% respectively.

MTT assay	DIP (μM)		H_20_2 (μM)	
	IC25	IC50	IC25	IC50
U87-MG	81	99	44	89
H4	57	66	31	63

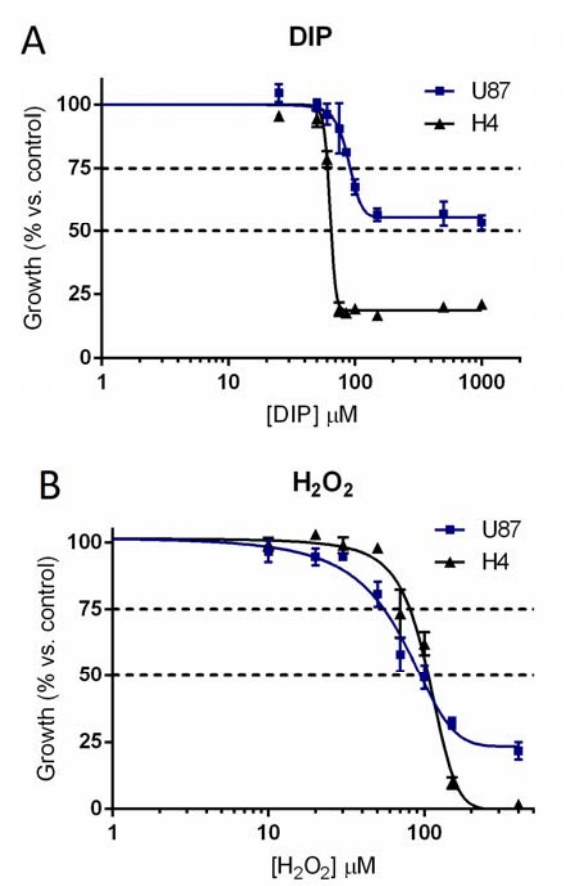

Figure 4: Dose-response curves from the cell counts using bright-field analysis. Cells were counted using bright-field microscopy on the 2nd day after the addition of stress factors in different concentrations. Cell counts of treated cells were divided with control counts, resulting in % of growth inhibition (y- axis), in (A) DIP- treated (x-axis) and (B) H_20_2-treated (x-axis) cells. . Data points represent mean values of triplicates in the experiment and error bars denote ± (SD) values. Dotted lines represent inhibitory concentrations IC25 and IC50 respectively.

lower concentration than DIP, which in fact does not inhibit cell growth completely (at least not in this concentration range). On the other hand, growth inhibition is more rapid

in DIP-treated cells compared to more gradual inhibition by H_20_2. Inhibitory concentrations (IC) were calculated from the plotted dose-response growth curves and they represent the effectiveness of a substance in inhibiting cell growth. IC25 and IC50 values, concentrations of a substance that inhibits cell growth for 25% and 50% respectively, were interpolated at Y=75 and Y=50 (Table 1). In line with the lower resistance of H4, the lower IC values of DIP and H_20_2 are needed to inhibit its cell growth for 25% and 50%.

Cell count by bright-field analysis with SpectraMax MiniMax 300 Imaging Cytometer resulted in rather divergent dose-response curves to that of MTT assay (Figure 4) due to high errors. One has to take into consideration that in higher concentrations of DIP and H_20_2, cells underwent cell death that was visible under bright-field microscope imaging, thus apoptotic bodies in a stain-free image lead to increasingly higher errors in the software automatized cell count with increasing concentrations of stress factors Dose-response curves for DIP-treatment have similar shapes and the trend between the two cell lines to that of MTT assay. Whereas the dose-response curves for H_20_2-treatment are not showing the same trend as in MTT assay due to the fact that the dead cells in the U87-MG cell line were still mostly attached and counted as alive. The IC values from that experiment were not calculated since the dose-response curves are not reliable enough due to high errors.

Cells morphology observations

Upon collection of the supernatants, cell images were routinely acquired. We noticed that U87-MG cells changed morphology when DIP-treated but not when H_20_2-treated. Normally, U87-MG cells are elongated but in mimicked hypoxia stress they shrank in size and looked rounded (Figure 5) which to our knowledge has not been known before. We have not observed that morphology change in H4 cell line.

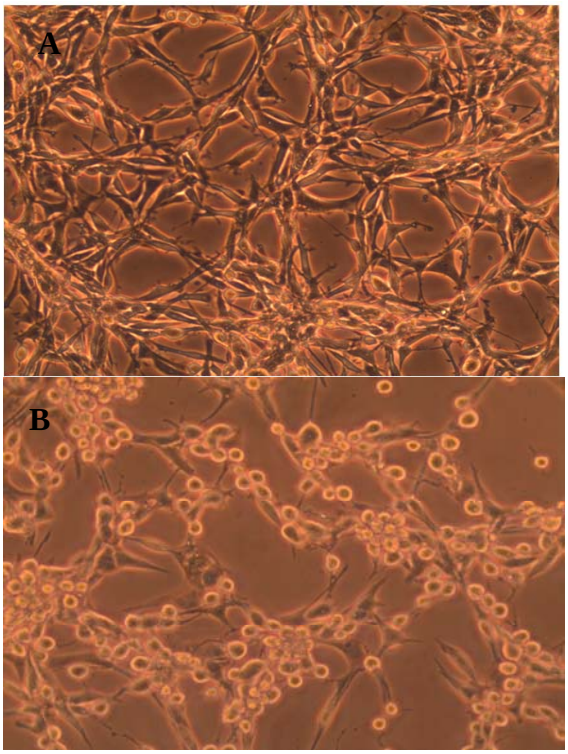

Figure 5: Morphology changes in DIP-treated U87-MG cells. Pictures were taken under 100 x magnifications with Leica objective on the day of exosomal collection in (A) control and (B) DIP-treated cells (48h exposure). DIP-treated cells changed the morphology from extended to rounded cells due to hypoxic stress.

Quantitative analysis of exosomes isolated from glioma cell lines under hypoxic and oxidative stress conditions.

Exosomes, isolated from U87-MG and H4 cell lines under two stress conditions (hypoxia and oxidative stress), were broken down and the total µg of proteins in the samples were measured with the BCA assay. The total mass of proteins in the samples was then divided by the number of cells present in the flasks on the day of collection in each condition. That calculation resulted in the measurement of µg of released proteins per million cells which was used to compare different samples among each other in terms of estimated exosome quantification. Three separate experiments have been done with both cell lines with the collection of exosomes from 10% dFBS medium under two stress conditions. In order to assess the influence of hypoxic and oxidative stress, preliminary IC25 concentrations of stress factors DIP and H_20_2 were used. The values

used in this set of experiments differ from the IC25 values reported in Table 1 as they were calculated from the initial MTT assays. Measurements of µg of released proteins per million cells are presented as separate experiments in Figure 6 where they correspond to the ones in Table 2.

There is no visible trend that the cells under stress conditions produced more exosomes than in control environment. In U87-MG cell line, two experiments showed slight decrease in the amount of exosomes released under hypoxia and slight increase of released exosomes in oxidative stress. On the other hand, the last experiment (sample 3) resulted in just the opposite trend. The amount of released proteins per million cells in the latter sample is also distinct from the other two experiments. Amounts of isolated exosomes in H4 cell line did not change drastically between the treatments with the exception of one peak in DIP-treated cells where was detected 2.7 fold increase in exosomes released per million cells. We also noticed that the confluency of cells may have an impact on the amount of released vesicles. Figure 6A and Table 2 show that when the U87-MG cells were fully confluent they

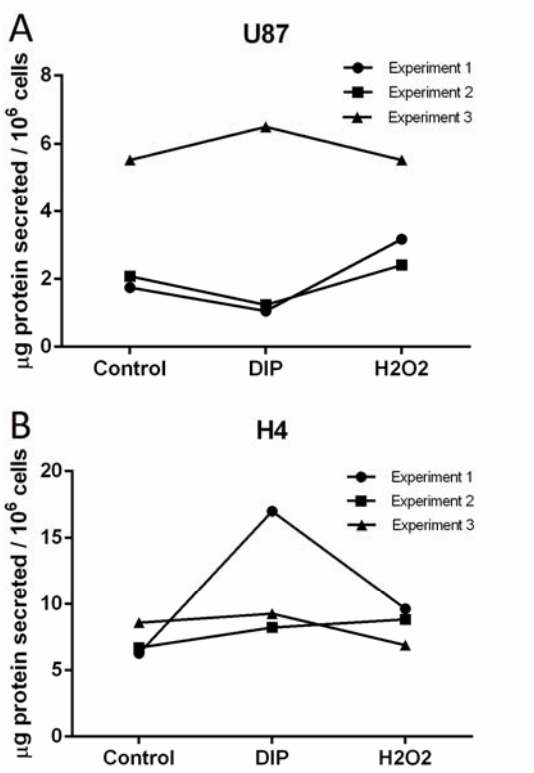

Figure 6: Quantification of exosomes with BCA protein measurements in three indiviual experiments. Graph shows µg of proteins secreted from 10^6 cells in control environment, hypoxia (DIP) and oxidative stress (H_20_2) in (A) U87-MG and (B) H4 cell lines. The experiments correspond to the ones in the Table 2. Experiment 1 from U87-MG cells was obtained from highly confluent cells and the rest were obtained from cells in medium confluency.

Table 2: Quantitative analyses of exosomes from U87-MG and H4 cells. Both cell lines were treated for 48 h with stress factors prior exosome collection. U87-MG cells were treated with 85 µM concentration of DIP and 70 µM concentration of H_20_2 while the H4 cells were treated with 60 (in 1st experiment) or 50 (in 2nd and 3rd experiment) µM concentration of DIP and 25 µM concentration of H_20_2. On the day of collection

U87- MG							
Experiment	Confluency	Control (in million cells)	% of control		µg protein secreted/ 106 cells (Control)	% of control	
			DIP	H202		DIP	H202
1	high	49,6	85 %	75 %	1,7	60 %	182 %
2	medium	33,2	81 %	82 %	2,1	59 %	116 %
3	medium	29,3	58 %	106 %	5,5	118 %	100 %
4	low	14,7	37 %		7,2	220 %	
5	low	13,5	63 %		4,1	290 %	

H4							
Experiment	Confluency	Control (in million cells)	% of control		µg protein secreted/ 106 cells (Control)	% of control	
			DIP	H202		DIP	H202
1	medium	13,3	28 %	72 %	6,3	271 %	154 %
2	medium	17,7	68 %	97 %	6,7	123 %	132 %
3	medium	12,6	74 %	116 %	8,6	108 %	80 %

produced considerably less exosomes as when in lower confluency with the exception of sample 3. For instance, U87-MG cells in low confluency (sample 4) in the control condition released vesicles accounting for 7.2 µg of proteins/10^6 cells which is around 3.7 fold increase than the cells in high confluency (Table 2). Also, in that sample we noticed that the cells in hypoxia stress produced 2.2 times more exosomes than in control (Table 2). We observed the same response from exosomes collected under serum free conditions (DMEM medium with B27 supplement and epidermal growth factor (EGF)). U87-MG cells produced 4.1 µg of proteins/10^6 cells (sample 5) in control, which accounts for a 2-fold increase compared to high confluent cells, and 2.9 times more in DIP-treated cells (Table 2).

NTA measurements of particle concentrations and size distributions of exosomal samples

Total particle concentration and size of six samples from H4 cell line (samples 2 and 3 in Table 2) were determined with the NTA. All the samples were frozen after exosome isolation at -80ºC until the NTA measurements. Numbers of particles per ml were converted to percentages of released vesicles in DIP and H_20_2-treated cells compared to control as an estimate of quantitative changes in production of exosomes. Percentages of released vesicles obtained from NTA measurements were differing on average by 18 % from the BCA measurements of total protein content (Figure 7), possibly indicating some protein contaminations in the exosomes samples. As a measurement related to sample purity the ratio of particle (in 10^{10}/ml) to protein (µg/ml) (Table 3) was calculated as proposed by a study from Webber *et al*. Ratio of $\geq 3\times10^{10}$ particles per µg of protein is proposed to be a measurement of high purity samples and a ratio of 1×10^{10} is proposed to contain around 50% of contaminant proteins (61). If our sample ratios are examined using that definition, then the samples are of medium or lower purity.

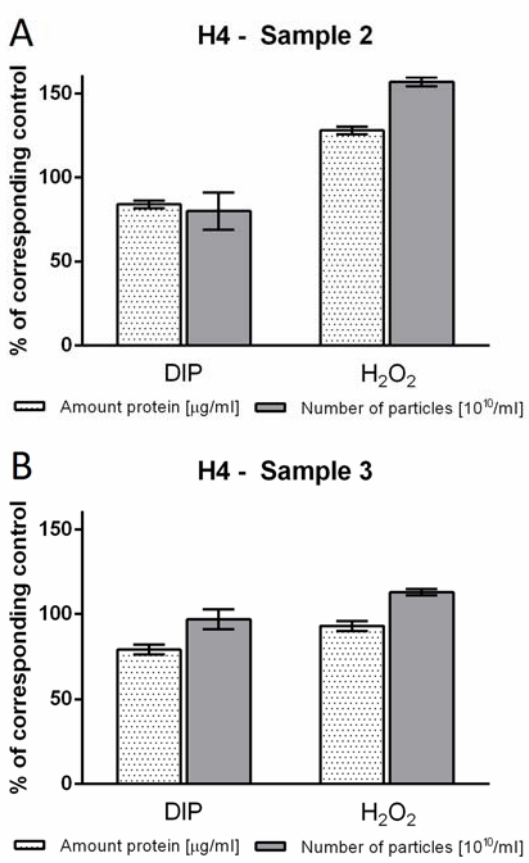

Figure 7: Comparison of percentages of cell-released particles from two stresses (hypoxia and oxidative stress) to control environment from the data obtained by two methods as a measurement of exosomal content. Amount of exosomes was measured as total protein content with BCA assay (light columns) and as a total amount of particles/ml with NTA (darker columns). The estimation of exosome amount is differing from one method to another in average of 18%.

Table 3: Exosome purity measurements from H4 cells using the ratio of particle to protein. The ratio is calculated from the particle count by Nanosight (10^{10} particles/ml) that is divided by the protein content (µg/ml) measured with BCA. It tells how pure the vesicles are with the determination of protein contaminants. The more contaminant proteins are there in the sample the lower ratio. According to Webber *et al*. the ratio of $3x10^{10}$ particles per µg of protein is considered as high purity sample and a ratio of 1×10^{10} is proposed to contain around 50% of contaminant proteins. Experiments correspond to the ones in Figure 6 and Table 2.

H4			
Experiment	Control	DIP	H202
2	1,57	1,50	1,93
3	1,70	2,09	2,07

Size distributions of samples were varying from 30-220 nm and the particle sizes were in most cases characterized by two or more peaks (graphs are not presented). The first peak was visible at 30-40 nm, the second at ca. 100 nm while the third one at ca. 200 nm. Shoulders in the distribution were also observed at higher sizes. Besides the probable presence of bigger vesicles than exosomes (above 200 nm) also the formation of particles aggregates and/or protein-particles might occur during freezing and thawing of samples.

High-throughput proteomic studies of exosomal proteome

Exosome proteomes, isolated from control and DIP-treated cells in B27+EGF medium (sample 5 in Table 2), were analyzed with the tandem mass spectrometry (MS/MS) using TMT. High-throughput proteomic study of control and DIP-treated sample triplicates resulted in the unambiguous detection of 441 proteins. In this set we found most of the known exosomal markers, such as CD63, CD9, CD82, HSP70, HSP90 and syntenin. We did not detect cell contaminant proteins Golgi apparatus (GA) marker GM130, mitochondrial marker VDAC1 and endoplasmatic reticulum (ER) marker calreticulin or calnexin. Among the detected proteins, 67 proteins had a significance value for the fold change of $p < 0.001$. The fold change of proteins in exosomes collected from DIP-treated cells compared to the control samples showed 33 proteins with fold changes with greater than two times. Among those, 11 proteins showed a decrease in fold change lower than 0.5 and 22 proteins higher than 2. These proteins were analyzed in the Database for Annotation, Visualization and Integrated Discovery (DAVID) respectively, resulting in different annotation clusters (62). Up-regulated proteins showed the cluster of ribosome proteins such as ribosomal subunits and ribonucleoproteins (Appendix 1). Instead, down-regulated proteins were clustered in cellular processes involved in the modulation of extracellular matrix. Among those were detected collagen, von Willebrand factor, cell adhesion proteins and extracellular matrix proteins (Appendix 2).

Discussion

Membrane vesicle trafficking is considered to be an important way of cell communication. Particularly exosomes are believed to play an important role as intercellular messengers since their cargo is believed to be packaged selectively in the vesicles (9, 14) and most cells in the human body appear to have a capability to release such vesicles. In this study, we set up a routine procedure of isolating and characterizing these vesicles. We also established a model for hypoxia and oxidative stress in two glioma cell lines in order to study whether the effect of such stressors has the impact on the release of exosomes in U87-MG and H4 cell lines. Here we present the preliminary data which does not show a notable trend in differential release of exosomes by cells in stress compared to control environment. However, we found initial evidence that the content of exosomes illustrate the metabolic state of donor cells.

The models of hypoxia and oxidative stress were assessed with the MTT assay and cell counts with bright-field analysis, resulting in dose-response curves of glioma cell lines (Figure 3 and Figure 4). Cell counts with bright-field analysis are in general very precise way of estimating cell viability. In our experiment however the cell counts were aggravated due to increased cell death at higher concentrations of stress factors. Floating apoptotic bodies gave a high background and the optical cytometer could not count with the same precision as when there was no or very little cell death, therefore the dose-response curves could be compromised. Since the experiment was repeated several times with the MTT assay and only one time with the bright-field cell counts, the former assay is more informative. These show that the two stress factors have different effectiveness on the growth

inhibition in cell lines. Hydrogen peroxide is more potent stress factor that elicited full effect at its high concentration compared to DIP that elicited a partial effect on growth inhibition. On the other hand, DIP had more abrupt effect (a steeper slope) with increasing concentrations than H_20_2 that induced a more gradual effect. DIP and H_20_2 stress factors affected H4 glioma cell line more strongly than the U87-MG cell line. Higher sensitivity of the H4 cell line could correlate to its lower malignant state compared to U87-MG. During the progression from low to high grade-malignancy many genetic alterations occur that contribute to higher resistant state of glioblastoma multiforme. These include stronger activation of growth signaling pathways involving EGFR, PTEN and Akt or genes that are involved in the cell cycle control such as p53 and Retinoblastoma which also decrease apoptosis rate (43).

For the induction of stress conditions in our experiments we decided to use IC25 values from MTT assay of stress factors in order to assess sufficient stress environment without inducing excessive cell death. During the apoptotic processes, cells start to condense and fragment, resulting in the release of apoptotic bodies, which carry all sorts of cell material. These vesicles can vary in size from 500-2000 nm (3) and their density can overlap with the exosomes which can cause problems during the isolation and analysis processes. This is a possible source of contamination in our experiments. Therefore the presence of such contaminants or any other possible unwanted impurities (e.g. microvesicles, protein aggregates) but also exosomal markers are usually routinely checked with Western blot. In our study, the proteomic analysis gives us first indication in this direction. Even though we did not find typical contaminants in the proteomics samples, the absence of these proteins in the mass spectrometry results does not allow to completely exclude possible impurities. The MS/MS technique detects only the proteins that are most abundant, therefore the contaminants might still be present in the sample but at lower concentrations (42). Nevertheless, among the detected proteins were for instance main exosomal markers, suggesting that exosomes represented a large part of our samples. However, further characterization steps are necessary, that will determine the purity of the exosome preparation. These for example include Western blot analysis for exosomal markers and contaminants, sucrose gradient centrifugation for confirmation of proper density and transmission electron microscopy (TEM) to morphologically confirm their identification as exosomes (32). In summary, we are confident from the NTA and MS/MS analyses that the particles we were analyzing were exosomes. But the extent of contamination remains somewhat unknown and more contamination might occur in samples where the cell death was increased. For example, in the sample 1 of H4 cell line (Figure 6, Table 2), there were only present 28% of cells in DIP- treated samples compared to control. This might not only reflect growth arrest but also cell death, resulting in such low cell numbers. Therefore, the exosomal fraction might also contain increased amount of apoptotic bodies, which in turn raised the count for µg of proteins release per million cells. Similarly, in DIP-treated U87-MG cells in experiment 4 (Table 2) we detected much more proteins released per million of cells compared to control (2.2 times more) while there was 63% decrease in cell growth. Hence, increase in released µg proteins/10^6 cells might not be due to greater cell-cell communication in stress conditions but rather due to contaminations from apoptotic bodies that gave false positive results.

Exosome concentration is very often measured as total protein content, present both in the core and in the lipid membrane, as a complementary measurement to the total particle concentration. In our experiments we analyzed exosomes mainly with the BCA to obtain measurements of total protein content as a determination of quantity changes in released vesicles in two stress conditions. We could observe some difference among

conditions, but not a notable trend. Further data collection and analysis are needed prior to drawing conclusions. The isolation of the exosomes constitutes a rather time consuming process, with materials yields being the main bottleneck in these studies. In future experiments we plan to scale up the amounts of cells and centrifugation volumes. From the data that we obtained we also noticed that cells which did not reach high confluency released more exosomes than very confluent cells. This might happen due to lower metabolism of confluent cells, which results in diminished cell signaling and metabolism. The result enables us to improve the cell densities used for harvest, hence the yield of pelleted material. By collecting the exosomes during the growing phase we also expect to improve reproducibility and facilitate data interpretation.

Comparison of particle concentrations from the NTA measurements with the protein amounts obtained with the BCA measurements suggests that the exosome samples 2 and 3 of H4 cell line were not highly purified. To improve the isolation and purification of exosomes, an additional washing step could be added in the process. This could improve the purity of the samples but would decrease the yield of isolated exosomes. According to the finding by Webber J. *et al.* (2013), the additional washing step might improve this ratio as little as 2-fold and therefore other approaches are more desired such as sucrose gradient centrifugation (61). The size distribution of particles in the sample showed that there was more than one peak in the size, which could be either due both to contaminations that occurred during sample preparation and to particles aggregation that might occur during freezing and thawing. We have noticed that if the samples were analyzed fresh, within few days after isolation, the size distribution was more consistent and did not show additional peaks in contrast to the samples that were analyzed after freezing and thawing.

It has been reported that exosomes from material of highly malignant glioblastoma patients and U87-MG glioma cell line are enriched in hypoxia-regulated proteins as for example matrix metalloproteinases, IL-8, PDGFs and caveolin 1(39). In our study we wanted to reproduce previously published results and examine whether U87-MG glioma cell line under DIP-induced hypoxia also produce exosomes enriched in angiogenic proteins. We however did not find any of these or other angiogenic proteins in hypoxic exosomes, possibly because the hypoxic stress on cells was not sufficient. DIP only mimics the HIF-1 response of hypoxia and other pathways involved in hypoxia may not be altered under DIP treatment. Moreover, to properly monitor cellular stress it would be interesting to look at the gene expression level of hypoxia-regulated genes, e.g. with real-time polymerase chain reaction (qPCR) or RNA microarrays. As a candidates could be for example chosen genes CA9 and EGFR, since the expression of both these genes is strongly connected with the HIF-1 activity (63, 64). However, DAVID functional annotation clustering of proteins with fold change of more than 2 in our experiment showed that these exosomes were enriched in ribosomal proteins and depleted in proteins involved in the modulation of extracellular matrix (ECM) compared to control exosomes. Explanation for this could be that the exosomes represent the intracellular cytoplasmic content of cells. Cells under stress become more metabolically active, resulting in increased ribosomal biogenesis (65) and therefore the higher enrichment of ribosomal proteins in exosomes might reflect increased cellular translation. However, depletion of ECM proteins might indicate a differential need for those proteins due to morphological changes that cells experience under hypoxic stress (Figure 5). DIP-treated cells became more rounded and therefore might not need as many cell adherent proteins as the normally shaped cells.

Conclusion

We set up the methods for exosomal isolation and two characterization techniques NTA and BCA. In all preparations that we analyzed we could confirm the presence of exosomes, however, verification of the purity of the exosomal samples remains an important issue. Further analysis will include Western Blots analysis of common contaminants, gradient centrifugations and TEM microscopy. Our data nevertheless show initial evidence that the exosome content reflects the inner metabolic status of cells. The study did not yet answer the question whether glioma cells exposed to hypoxic and oxidative stress produce more exosomes than the cells in standard culture conditions and more experiments are needed before making final conclusions.

Acknowledgments

I thank V. Claudio for help with the Nanoparticle track analyses and bright-field analyses with SpectraMax MiniMax 300 Imaging Cytometer. Also, I would like to thank Proteomic Core Facility at Sahlgrenska academy, Gothenburg University, for performing MS/MS analysis. Last but not least, I thank G.Kuhn and V.Claudio for guidance through this study.

References

1. Alberts B, Johnson A, *et al.* Molecular Biology of the Cell. 5th ed: Garland Science; 2007.
2. Pan BT, Johnstone RM. Fate of the transferrin receptor during maturation of sheep reticulocytes invitro - selective externalization of the receptor. Cell. 1983;33(3):967-977.
3. Andaloussi S, Mager I, *et al.* Extracellular vesicles: biology and emerging therapeutic opportunities. Nat Rev Drug Discov. 2013;12(5):347-357.
4. [25.11.2014]. Available from: http://www.nobelprize.org/nobel_prizes/medicine/laureates/2013/press.html.
5. D'Souza-Schorey C, Clancy JW. Tumor-derived microvesicles: shedding light on novel microenvironment modulators and prospective cancer biomarkers. Gene Dev. 2012;26(12):1287-1299.
6. Distler JH, Pisetsky DS, *et al.* Microparticles as regulators of inflammation: novel players of cellular crosstalk in the rheumatic diseases. Arthritis Rheum. 2005;52(11):3337-3348.
7. Denzer K, Kleijmeer MJ, *et al.* Exosome: from internal vesicle of the multivesicular body to intercellular signaling device. J Cell Sci. 2000;113(19):3365-3374.
8. Thery C, Zitvogel L, *et al.* Exosomes: Composition, biogenesis and function. Nat Rev Immunol. 2002;2(8):569-579.
9. Skog J, Wurdinger T, *et al.* Glioblastoma microvesicles transport RNA and proteins that promote tumour growth and provide diagnostic biomarkers. Nat Cell Biol. 2008;10(12):1470-U1209.
10. Waldenstrom A, Ronquist G. Role of exosomes in myocardial remodeling. Circ Res. 2014;114(2):315-324.
11. Johnstone RM, Adam M, *et al.* Vesicle formation during reticulocyte maturation - association of plasma-membrane activities with released vesicles (exosomes). J Biol Chem. 1987;262(19):9412-9420.
12. Bang C, Thum T. Exosomes: New players in cell-cell communication. Int J Biochem Cell B. 2012;44(11):2060-2064.
13. Raposo G, Nijman HW, *et al.* B lymphocytes secrete antigen-presenting vesicles. J Exp Med. 1996;183(3):1161-1172.
14. Valadi H, Ekstrom K, *et al.* Exosome-mediated transfer of mRNAs and microRNAs is a novel mechanism of genetic exchange between cells. Nat Cell Biol. 2007;9(6):654-U672.
15. Jenjaroenpun P, Kremenska Y, *et al.* Characterization of RNA in exosomes secreted by human breast cancer cell lines using next-generation sequencing. PeerJ. 2013;1:e201.
16. Guescini M, Genedani S, *et al.* Astrocytes and Glioblastoma cells release

exosomes carrying mtDNA. J Neural Transm. 2010;117(1):1-4.
17. Mittelbrunn M, Gutierrez-Vazquez C, *et al.* Unidirectional transfer of microRNA-loaded exosomes from T cells to antigen-presenting cells. Nat Commun. 2011;2:282.
18. Svensson KJ, Kucharzewska P, *et al.* Hypoxia triggers a proangiogenic pathway involving cancer cell microvesicles and PAR-2-mediated heparin-binding EGF signaling in endothelial cells. P Natl Acad Sci USA. 2011;108(32):13147-13152.
19. Eldh M, Ekstrom K, *et al.* Exosomes communicate protective messages during oxidative stress; possible role of exosomal shuttle RNA. Plos One. 2010;5(12).
20. Segura E, Guerin C, *et al.* CD8(+) dendritic cells use LFA-1 to capture MHC-peptide complexes from exosomes in vivo. J Immunol. 2007;179(3):1489-1496.
21. Morelli AE, Larregina AT, *et al.* Endocytosis, intracellular sorting, and processing of exosomes by dendritic cells. Blood. 2004;104(10):3257-3266.
22. Lai CP, Breakefield XO. Role of exosomes/microvesicles in the nervous system and use in emerging therapies. Front Physiol. 2012;3:228.
23. Potolicchio A, Carven GJ, *et al.* Proteomic analysis of microglia-derived exosomes: Metabolic role of the aminopeptidase CD13 in neuropeptide catabolism. J Immunol. 2005;175(4):2237-2243.
24. Kramer-Albers EM, Bretz N, *et al.* Oligodendrocytes secrete exosomes containing major myelin and stress-protective proteins: Trophic support for axons? Proteom Clin Appl. 2007;1(11):1446-1461.
25. Faure J, Lachenal G, *et al.* Exosomes are released by cultured cortical neurones. Mol Cell Neurosci. 2006;31(4):642-648.
26. Sims B, Gu L, *et al.* Neural stem cell-derived exosomes mediate viral entry. Int J Nanomedicine. 2014;9:4893-4897.
27. Skokos D, Le Panse S, *et al.* Mast cell-dependent B and T lymphocyte activation is mediated by the secretion of immunologically active exosomes. J Immunol. 2001;166(2):868-876.
28. Hood JL, Pan H, *et al.* Paracrine induction of endothelium by tumor exosomes. Lab Invest. 2009;89(11):1317-1328.
29. Simpson RJ, Jensen SS, *et al.* Proteomic profiling of exosomes: current perspectives. Proteomics. 2008;8(19):4083-4099.
30. Kooijmans SA, Vader P, *et al.* Exosome mimetics: a novel class of drug delivery systems. Int J Nanomedicine. 2012;7:1525-1541.
31. van den Boorn JG, Schlee M, *et al.* SiRNA delivery with exosome nanoparticles. Nat Biotechnol. 2011;29(4):325-326.
32. Thery C, Amigorena S, *et al.* Isolation and characterization of exosomes from cell culture supernatants and biological fluids. Curr Protoc Cell Biol. 2006;Chapter 3:Unit 3 22.
33. Tauro BJ, Greening DW, *et al.* Comparison of ultracentrifugation, density gradient separation, and immunoaffinity capture methods for isolating human colon cancer cell line LIM1863-derived exosomes. Methods. 2012;56(2):293-304.
34. Vlassov AV, Magdaleno S, *et al.* Exosomes: current knowledge of their composition, biological functions, and diagnostic and therapeutic potentials. Biochim Biophys Acta. 2012;1820(7):940-948.
35. Van Rooijen N, Sanders A. Liposome mediated depletion of macrophages: mechanism of action, preparation of liposomes and applications. J Immunol Methods. 1994;174(1-2):83-93.
36. Dragovic RA, Gardiner C, *et al.* Sizing and phenotyping of cellular vesicles using Nanoparticle Tracking Analysis. Nanomedicine. 2011;7(6):780-788.
37. Svensson KJ, Christianson HC, *et al.* Exosome uptake depends on ERK1/2-Heat Shock Protein 27 signaling and lipid raft-mediated endocytosis negatively regulated by Caveolin-1. J Biol Chem. 2013;288(24):17713-17724.
38. Sapan CV, Lundblad RL, *et al.* Colorimetric protein assay techniques.

Biotechnol Appl Biochem. 1999;29 (Pt 2):99-108.
39. Kucharzewska P, Christianson HC, *et al.* Exosomes reflect the hypoxic status of glioma cells and mediate hypoxia-dependent activation of vascular cells during tumor development. Proc Natl Acad Sci U S A. 2013;110(18):7312-7317.
40. Lasser C, Eldh M, *et al.* Isolation and characterization of RNA-containing exosomes. J Vis Exp. 2012(59):e3037.
41. Burnette WN. "Western blotting": electrophoretic transfer of proteins from sodium dodecyl sulfate--polyacrylamide gels to unmodified nitrocellulose and radiographic detection with antibody and radioiodinated protein A. Anal Biochem. 1981;112(2):195-203.
42. Nesvizhskii AI, Keller A, *et al.* A statistical model for identifying proteins by tandem mass spectrometry. Anal Chem. 2003;75(17):4646-4658.
43. Louis DN. Molecular pathology of malignant gliomas. Annu Rev Pathol. 2006;1:97-117.
44. Niu W, Zang T, *et al.* In vivo reprogramming of astrocytes to neuroblasts in the adult brain. Nat Cell Biol. 2013;15(10):1164-1175.
45. Rong Y, Durden DL, *et al.* 'Pseudopalisading' necrosis in glioblastoma: a familiar morphologic feature that links vascular pathology, hypoxia, and angiogenesis. J Neuropathol Exp Neurol. 2006;65(6):529-539.
46. Clark MJ, Homer N, *et al.* U87MG decoded: the genomic sequence of a cytogenetically aberrant human cancer cell line. PLoS Genet. 2010;6(1):e1000832.
47. Krex D, Mohr B, *et al.* Identification of uncommon chromosomal aberrations in the neuroglioma cell line H4 by spectral karyotyping. J Neurooncol. 2001;52(2):119-128.
48. Fischer I, Gagner JP, *et al.* Angiogenesis in gliomas: biology and molecular pathophysiology. Brain Pathol. 2005;15(4):297-310.
49. Kaur B, Khwaja FW, *et al.* Hypoxia and the hypoxia-inducible-factor pathway in glioma growth and angiogenesis. Neuro Oncol. 2005;7(2):134-153.
50. Semenza GL. HIF-1, O(2), and the 3 PHDs: how animal cells signal hypoxia to the nucleus. Cell. 2001;107(1):1-3.
51. Hanahan D, Weinberg RA. Hallmarks of cancer: the next generation. Cell. 2011;144(5):646-674.
52. Weis SM, Cheresh DA. Tumor angiogenesis: molecular pathways and therapeutic targets. Nat Med. 2011;17(11):1359-1370.
53. King HW, Michael MZ, *et al.* Hypoxic enhancement of exosome release by breast cancer cells. BMC cancer. 2012;12:421.
54. Wu D, Yotnda P. Induction and testing of hypoxia in cell culture. J Vis Exp. 2011(54).
55. Ruas JL, Berchner-Pfannschmidt U, *et al.* Complex regulation of the transactivation function of hypoxia-inducible factor-1 alpha by direct interaction with two distinct domains of the CREB-binding protein/p300. J Biol Chem. 2010;285(4):2601-2609.
56. Kallio PJ, Wilson WJ, *et al.* Regulation of the hypoxia-inducible transcription factor 1alpha by the ubiquitin-proteasome pathway. J Biol Chem. 1999;274(10):6519-6525.
57. Nandal A, Ruiz JC, *et al.* Activation of the HIF prolyl hydroxylase by the iron chaperones PCBP1 and PCBP2. Cell Metab. 2011;14(5):647-657.
58. Martindale JL, Holbrook NJ. Cellular response to oxidative stress: signaling for suicide and survival. J Cell Physiol. 2002;192(1):1-15.
59. Chen ZH, Yoshida Y, *et al.* Adaptation to hydrogen peroxide enhances PC12 cell tolerance against oxidative damage. Neurosci Lett. 2005;383(3):256-259.
60. Wisniewski JR, Zougman A, *et al.* Universal sample preparation method for proteome analysis. Nat Methods. 2009;6(5):359-362.
61. Webber J, Clayton A. How pure are your vesicles? J Extracell Vesicles. 2013;2.
62. Dennis G, Jr., Sherman BT, *et al.* DAVID: Database for Annotation, Visualization, and Integrated Discovery. Genome Biol. 2003;4(5):P3.

63. Kaluz S, Kaluzova M, *et al.* Transcriptional control of the tumor- and hypoxia-marker carbonic anhydrase 9: A one transcription factor (HIF-1) show? Biochim Biophys Acta. 2009;1795(2):162-172.
64. Franovic A, Gunaratnam L, *et al.* Translational up-regulation of the EGFR by tumor hypoxia provides a nonmutational explanation for its overexpression in human cancer. Proc Natl Acad Sci U S A. 2007;104(32):13092-13097.
65. Liu L, Cash TP, *et al.* Hypoxia-induced energy stress regulates mRNA translation and cell growth. Mol Cell. 2006;21(4):521-531.

Supplementary information

Appendix 1: 22 proteins with the fold change of more than 2 were analyzed in DAVID database resulting in 11 clusters. Count is representing number of proteins involved in the different processes in the cell or cellular part. P-value and Benjamini are the statistical measurements of significance where the lower number means higher significance.

Proteins with fold change more than 2				
22 DAVID IDs				
Annotation Cluster 1	**Enrichment Score: 7.22**	**Count**	**P_Value**	**Benjamini**
SP_PIR_KEYWORDS	ribonucleoprotein	12	1.5E-15	9.5E-14
GOTERM_BP_ALL	translational elongation	8	5.6E-11	1.6E-8
SP_PIR_KEYWORDS	ribosome	7	1.3E-10	2.6E-9
GOTERM_CC_ALL	cytosolic ribosome	7	5.3E-10	2.0E-8
SP_PIR_KEYWORDS	protein biosynthesis	8	7.9E-10	1.2E-8
SP_PIR_KEYWORDS	ribosomal protein	8	7.9E-10	1.2E-8
KEGG_PATHWAY	Ribosome	8	1.0E-9	7.3E-9
GOTERM_MF_ALL	structural constituent of ribosome	8	1.9E-9	7.2E-8
GOTERM_CC_ALL	ribosome	8	5.0E-9	9.2E-8
GOTERM_BP_ALL	translation	9	8.3E-9	1.2E-6
GOTERM_CC_ALL	cytosolic large ribosomal subunit	5	1.3E-7	1.6E-6
GOTERM_CC_ALL	ribosomal subunit	6	4.4E-7	4.6E-6
GOTERM_CC_ALL	cytosolic part	6	1.0E-6	7.6E-6
GOTERM_CC_ALL	large ribosomal subunit	5	1.3E-6	8.9E-6
GOTERM_MF_ALL	structural molecule activity	8	1.5E-5	2.9E-4
GOTERM_CC_ALL	cytosol	9	1.2E-4	7.3E-4
GOTERM_BP_ALL	cellular protein metabolic process	10	2.8E-3	5.6E-2
GOTERM_CC_ALL	cytoplasmic part	13	6.4E-3	2.5E-2
GOTERM_BP_ALL	protein metabolic process	10	9.7E-3	1.5E-1
Annotation Cluster 2	**Enrichment Score: 6.45**	**Count**	**P_Value**	**Benjamini**
GOTERM_CC_ALL	ribonucleoprotein complex	15	3.7E-17	2.8E-15
GOTERM_CC_ALL	macromolecular complex	18	6.7E-10	1.7E-8
GOTERM_CC_ALL	non-membrane-bounded organelle	16	1.0E-8	1.5E-7
GOTERM_CC_ALL	intracellular non-membrane-bounded organelle	16	1.0E-8	1.5E-7
GOTERM_CC_ALL	intracellular organelle	19	1.4E-3	7.3E-3
GOTERM_CC_ALL	organelle	19	1.4E-3	6.9E-3
GOTERM_CC_ALL	cytoplasmic part	13	6.4E-3	2.5E-2
GOTERM_CC_ALL	cytoplasm	16	8.2E-3	2.9E-2
Annotation Cluster 3	**Enrichment Score: 4.2**	**Count**	**P_Value**	**Benjamini**
GOTERM_CC_ALL	macromolecular complex	18	6.7E-10	1.7E-8
SP_PIR_KEYWORDS	acetylation	16	2.6E-9	3.2E-8
GOTERM_BP_ALL	translation	9	8.3E-9	1.2E-6
GOTERM_BP_ALL	gene expression	17	3.3E-8	3.2E-6
GOTERM_CC_ALL	intracellular organelle part	17	9.3E-7	8.6E-6
GOTERM_CC_ALL	organelle part	17	1.0E-6	8.3E-6

GOTERM_BP_ALL	cellular macromolecule biosynthetic process	14	1.4E-5	1.0E-3
GOTERM_BP_ALL	macromolecule biosynthetic process	14	1.5E-5	8.8E-4
GOTERM_BP_ALL	cellular macromolecule metabolic process	17	1.0E-4	4.3E-3
GOTERM_CC_ALL	cytosol	9	1.2E-4	7.3E-4
GOTERM_BP_ALL	cellular biosynthetic process	14	1.4E-4	4.9E-3
GOTERM_BP_ALL	biosynthetic process	14	1.9E-4	6.0E-3
GOTERM_BP_ALL	macromolecule metabolic process	17	3.7E-4	9.5E-3
GOTERM_CC_ALL	intracellular organelle	19	1.4E-3	7.3E-3
GOTERM_CC_ALL	organelle	19	1.4E-3	6.9E-3
GOTERM_BP_ALL	cellular metabolic process	17	2.7E-3	5.7E-2
GOTERM_BP_ALL	cellular protein metabolic process	10	2.8E-3	5.6E-2
GOTERM_CC_ALL	intracellular part	20	3.4E-3	1.5E-2
GOTERM_BP_ALL	primary metabolic process	17	4.6E-3	8.4E-2
GOTERM_CC_ALL	intracellular	20	6.1E-3	2.5E-2
GOTERM_BP_ALL	protein metabolic process	10	9.7E-3	1.5E-1
GOTERM_BP_ALL	metabolic process	17	1.6E-2	1.9E-1
GOTERM_BP_ALL	cellular process	19	8.6E-2	5.9E-1
Annotation Cluster 4	**Enrichment Score: 2.81**	**Count**	**P_Value**	**Benjamini**
GOTERM_BP_ALL	RNA processing	7	8.0E-5	3.8E-3
GOTERM_BP_ALL	RNA metabolic process	8	2.0E-4	5.7E-3
GOTERM_BP_ALL	RNA splicing, via transesterification reactions	4	1.2E-3	2.9E-2
GOTERM_BP_ALL	RNA splicing, via transesterification reactions with bulged adenosine as nucleophile	4	1.2E-3	2.9E-2
GOTERM_BP_ALL	nuclear mRNA splicing, via spliceosome	4	1.2E-3	2.9E-2
GOTERM_BP_ALL	RNA splicing	4	7.1E-3	1.2E-1
GOTERM_BP_ALL	mRNA processing	4	1.0E-2	1.5E-1
GOTERM_BP_ALL	mRNA metabolic process	4	1.5E-2	1.9E-1
Annotation Cluster 5	**Enrichment Score: 2.78**	**Count**	**P_Value**	**Benjamini**
GOTERM_CC_ALL	macromolecular complex	18	6.7E-10	1.7E-8
GOTERM_MF_ALL	protein binding	20	3.9E-4	6.0E-3
GOTERM_CC_ALL	intracellular part	20	3.4E-3	1.5E-2
GOTERM_CC_ALL	intracellular	20	6.1E-3	2.5E-2
GOTERM_MF_ALL	binding	21	1.0E-1	5.2E-1
GOTERM_CC_ALL	cell part	21	2.4E-1	5.1E-1
GOTERM_CC_ALL	cell	21	2.4E-1	5.0E-1
Annotation Cluster 6	**Enrichment Score: 2.76**	**Count**	**P_Value**	**Benjamini**
INTERPRO	Nucleotide-binding, alpha-beta plait	5	1.3E-4	8.0E-3
SMART	RRM	4	1.8E-3	1.9E-2
INTERPRO	RNA recognition motif, RNP-1	4	2.3E-3	6.6E-2
UP_SEQ_FEATURE	domain:RRM 2	3	5.4E-3	4.0E-1
UP_SEQ_FEATURE	domain:RRM 1	3	5.4E-3	4.0E-1
Annotation Cluster 7	**Enrichment Score: 2.34**	**Count**	**P_Value**	**Benjamini**
GOTERM_BP_ALL	RNA processing	7	8.0E-5	3.8E-3
GOTERM_BP_ALL	ncRNA processing	3	2.8E-2	3.0E-1

GOTERM_BP_ALL	ncRNA metabolic process	3	4.1E-2	3.7E-1
Annotation Cluster 8	**Enrichment Score: 1.28**	**Count**	**P_Value**	**Benjamini**
GOTERM_BP_ALL	ribosome biogenesis	3	1.3E-2	1.8E-1
GOTERM_BP_ALL	ribonucleoprotein complex biogenesis	3	2.6E-2	2.9E-1
GOTERM_BP_ALL	cellular component biogenesis	3	4.2E-1	9.8E-1
Annotation Cluster 9	**Enrichment Score: 0.85**	**Count**	**P_Value**	**Benjamini**
GOTERM_CC_ALL	nuclear part	10	1.7E-4	9.7E-4
GOTERM_CC_ALL	nucleolus	6	1.4E-3	6.6E-3
GOTERM_MF_ALL	nucleotide binding	10	1.8E-3	2.3E-2
GOTERM_CC_ALL	nuclear lumen	7	7.2E-3	2.6E-2
SMART	AAA	3	1.3E-2	6.7E-2
INTERPRO	ATPase, AAA+ type, core	3	1.4E-2	2.5E-1
GOTERM_CC_ALL	intracellular organelle lumen	7	1.9E-2	6.2E-2
UP_SEQ_FEATURE	nucleotide phosphate-binding region:ATP	5	1.9E-2	5.9E-1
GOTERM_CC_ALL	organelle lumen	7	2.1E-2	6.6E-2
GOTERM_CC_ALL	membrane-enclosed lumen	7	2.3E-2	6.9E-2
SP_PIR_KEYWORDS	nucleus	10	2.8E-2	2.2E-1
GOTERM_BP_ALL	DNA replication	3	2.9E-2	3.0E-1
GOTERM_BP_ALL	nucleobase, nucleoside, nucleotide and nucleic acid metabolic process	10	3.3E-2	3.2E-1
GOTERM_BP_ALL	cellular nitrogen compound metabolic process	10	5.1E-2	4.3E-1
SP_PIR_KEYWORDS	atp-binding	5	5.2E-2	3.1E-1
GOTERM_BP_ALL	nitrogen compound metabolic process	10	6.1E-2	4.7E-1
GOTERM_CC_ALL	nucleus	11	7.1E-2	1.9E-1
GOTERM_MF_ALL	nucleoside-triphosphatase activity	4	7.7E-2	5.9E-1
GOTERM_MF_ALL	pyrophosphatase activity	4	8.5E-2	5.7E-1
GOTERM_MF_ALL	hydrolase activity, acting on acid anhydrides, in phosphorus-containing anhydrides	4	8.6E-2	5.3E-1
GOTERM_MF_ALL	hydrolase activity, acting on acid anhydrides	4	8.7E-2	5.0E-1
GOTERM_CC_ALL	nucleoplasm	4	9.6E-2	2.5E-1
SP_PIR_KEYWORDS	nucleotide-binding	5	1.1E-1	5.0E-1
GOTERM_MF_ALL	ATP binding	5	1.4E-1	6.3E-1
GOTERM_MF_ALL	adenyl ribonucleotide binding	5	1.5E-1	6.1E-1
GOTERM_BP_ALL	DNA metabolic process	3	1.6E-1	8.1E-1
GOTERM_MF_ALL	adenyl nucleotide binding	5	1.7E-1	6.4E-1
GOTERM_MF_ALL	purine nucleoside binding	5	1.8E-1	6.3E-1
GOTERM_MF_ALL	nucleoside binding	5	1.8E-1	6.1E-1
GOTERM_BP_ALL	regulation of gene expression	7	2.0E-1	8.8E-1
GOTERM_MF_ALL	ribonucleotide binding	5	2.5E-1	7.2E-1
GOTERM_MF_ALL	purine ribonucleotide binding	5	2.5E-1	7.2E-1
GOTERM_MF_ALL	purine nucleotide binding	5	2.7E-1	7.4E-1
GOTERM_BP_ALL	cell cycle	3	3.0E-1	9.6E-1
GOTERM_BP_ALL	regulation of macromolecule metabolic process	7	3.1E-1	9.6E-1
GOTERM_BP_ALL	regulation of primary metabolic process	7	3.2E-1	9.6E-1

SP_PIR_KEYWORDS	dna-binding	4	3.3E-1	8.7E-1
GOTERM_BP_ALL	regulation of cellular metabolic process	7	3.6E-1	9.8E-1
GOTERM_BP_ALL	regulation of nucleobase, nucleoside, nucleotide and nucleic acid metabolic process	6	3.7E-1	9.7E-1
GOTERM_BP_ALL	regulation of nitrogen compound metabolic process	6	3.8E-1	9.7E-1
GOTERM_BP_ALL	regulation of metabolic process	7	4.1E-1	9.8E-1
GOTERM_CC_ALL	protein complex	5	4.1E-1	7.1E-1
GOTERM_CC_ALL	intracellular membrane-bounded organelle	12	4.2E-1	7.0E-1
GOTERM_CC_ALL	membrane-bounded organelle	12	4.2E-1	6.9E-1
GOTERM_BP_ALL	transcription	4	5.9E-1	1.0E0
GOTERM_BP_ALL	regulation of macromolecule biosynthetic process	5	5.9E-1	1.0E0
GOTERM_BP_ALL	regulation of cellular biosynthetic process	5	6.3E-1	1.0E0
GOTERM_BP_ALL	regulation of biosynthetic process	5	6.3E-1	1.0E0
GOTERM_MF_ALL	hydrolase activity	4	6.3E-1	9.8E-1
GOTERM_MF_ALL	DNA binding	4	6.5E-1	9.8E-1
SP_PIR_KEYWORDS	transcription regulation	3	6.6E-1	9.9E-1
SP_PIR_KEYWORDS	Transcription	3	6.8E-1	9.9E-1
GOTERM_BP_ALL	regulation of transcription	4	7.4E-1	1.0E0
GOTERM_BP_ALL	regulation of RNA metabolic process	3	7.5E-1	1.0E0
GOTERM_MF_ALL	catalytic activity	7	7.8E-1	1.0E0
GOTERM_BP_ALL	biological regulation	10	8.3E-1	1.0E0
GOTERM_BP_ALL	regulation of cellular process	9	8.3E-1	1.0E0
GOTERM_BP_ALL	regulation of biological process	9	8.8E-1	1.0E0
SP_PIR_KEYWORDS	alternative splicing	6	9.5E-1	1.0E0
UP_SEQ_FEATURE	splice variant	6	9.6E-1	1.0E0
GOTERM_BP_ALL	response to stimulus	3	9.7E-1	1.0E0
Annotation Cluster 10	**Enrichment Score: 0.69**	**Count**	**P_Value**	**Benjamini**
GOTERM_CC_ALL	cytoskeletal part	4	1.1E-1	2.8E-1
GOTERM_CC_ALL	microtubule cytoskeleton	3	1.5E-1	3.5E-1
GOTERM_CC_ALL	cytoskeleton	4	2.5E-1	4.9E-1
GOTERM_CC_ALL	protein complex	5	4.1E-1	7.1E-1
Annotation Cluster 11	**Enrichment Score: 0.12**	**Count**	**P_Value**	**Benjamini**
GOTERM_BP_ALL	anatomical structure morphogenesis	3	5.2E-1	9.9E-1
GOTERM_BP_ALL	anatomical structure development	3	9.0E-1	1.0E0
GOTERM_BP_ALL	developmental process	3	9.6E-1	1.0E0

Appendix 2: 11 proteins with the fold change of less than 0.5 were analyzed in DAVID database resulting in 10 clusters. Count is representing number of proteins involved in the different processes in the cell or cellular part. P-value and Benjamini are the statistical measurements of significance where the lower number means higher significance.

Proteins with fold change of less than 0.5				
11 DAVID IDs				
Annotation Cluster 1	**Enrichment Score: 3.16**	**Count**	**P_Value**	**Benjamini**
OMIM_DISEASE	Ullrich congenital muscular dystrophy	3	2.7E-6	2.4E-5
OMIM_DISEASE	Bethlem myopathy	3	2.7E-6	2.4E-5
PIR_SUPERFAMILY	PIRSF002259:collagen VI	3	3.9E-6	3.2E-5
UP_SEQ_FEATURE	domain:VWFA 3	3	5.2E-6	5.8E-4
SP_PIR_KEYWORDS	cell binding	3	2.5E-5	1.7E-3
UP_SEQ_FEATURE	domain:VWFA 1	3	2.9E-5	1.6E-3
GOTERM_CC_ALL	proteinaceous extracellular matrix	5	3.1E-5	2.2E-3
UP_SEQ_FEATURE	domain:VWFA 2	3	3.3E-5	1.2E-3
GOTERM_CC_ALL	extracellular matrix	5	4.1E-5	1.5E-3
UP_SEQ_FEATURE	region of interest:Triple-helical region	3	6.2E-5	1.7E-3
SP_PIR_KEYWORDS	trimer	3	7.9E-5	2.6E-3
SP_PIR_KEYWORDS	hydroxylysine	3	1.1E-4	2.5E-3
SP_PIR_KEYWORDS	triple helix	3	1.1E-4	2.5E-3
SP_PIR_KEYWORDS	hydroxyproline	3	1.6E-4	2.7E-3
SP_PIR_KEYWORDS	extracellular matrix	4	2.2E-4	2.9E-3
SP_PIR_KEYWORDS	pyroglutamic acid	3	2.5E-4	2.8E-3
SP_PIR_KEYWORDS	hydroxylation	3	5.9E-4	5.0E-3
GOTERM_CC_ALL	sarcolemma	3	7.7E-4	1.9E-2
SP_PIR_KEYWORDS	Secreted	6	9.0E-4	6.7E-3
UP_SEQ_FEATURE	short sequence motif:Cell attachment site	3	9.2E-4	1.5E-2
INTERPRO	von Willebrand factor, type A	3	9.7E-4	3.6E-2
SP_PIR_KEYWORDS	blocked amino end	3	9.9E-4	6.6E-3
SP_PIR_KEYWORDS	collagen	3	1.1E-3	6.4E-3
INTERPRO	Collagen triple helix repeat	3	1.1E-3	2.1E-2
SMART	VWA	3	1.5E-3	1.5E-2
GOTERM_CC_ALL	extracellular region part	5	2.1E-3	2.5E-2
KEGG_PATHWAY	ECM-receptor interaction	3	3.9E-3	4.9E-2
GOTERM_CC_ALL	extracellular region	6	4.7E-3	4.8E-2
UP_SEQ_FEATURE	glycosylation site:N-linked (GlcNAc...)	7	9.5E-3	1.2E-1
SP_PIR_KEYWORDS	glycoprotein	7	1.1E-2	5.8E-2
SP_PIR_KEYWORDS	cell adhesion	3	1.9E-2	8.9E-2
KEGG_PATHWAY	Focal adhesion	3	2.1E-2	1.3E-1
SP_PIR_KEYWORDS	disease mutation	4	4.4E-2	1.8E-1
GOTERM_BP_ALL	cell adhesion	3	5.6E-2	1.0E0
GOTERM_BP_ALL	biological adhesion	3	5.6E-2	9.9E-1
GOTERM_CC_ALL	extracellular space	3	6.6E-2	2.8E-1
SP_PIR_KEYWORDS	coiled coil	4	7.9E-2	2.9E-1

GOTERM_CC_ALL	plasma membrane	4	4.4E-1	8.0E-1
Annotation Cluster 2	**Enrichment Score: 2.03**	**Count**	**P_Value**	**Benjamini**
SP_PIR_KEYWORDS	signal	8	2.9E-4	2.8E-3
UP_SEQ_FEATURE	signal peptide	8	3.0E-4	6.8E-3
SP_PIR_KEYWORDS	Secreted	6	9.0E-4	6.7E-3
GOTERM_CC_ALL	extracellular region	6	4.7E-3	4.8E-2
SP_PIR_KEYWORDS	polymorphism	9	1.7E-1	5.2E-1
UP_SEQ_FEATURE	sequence variant	9	2.2E-1	9.3E-1
GOTERM_MF_ALL	binding	10	4.6E-1	1.0E0
Annotation Cluster 3	**Enrichment Score: 1.6**	**Count**	**P_Value**	**Benjamini**
UP_SEQ_FEATURE	short sequence motif:Prevents secretion from ER	3	4.1E-4	7.7E-3
GOTERM_CC_ALL	endoplasmic reticulum lumen	3	1.1E-3	2.0E-2
GOTERM_CC_ALL	pigment granule	3	1.4E-3	2.0E-2
GOTERM_CC_ALL	melanosome	3	1.4E-3	2.0E-2
SP_PIR_KEYWORDS	endoplasmic reticulum	4	5.0E-3	2.8E-2
GOTERM_CC_ALL	endoplasmic reticulum part	3	1.9E-2	1.6E-1
GOTERM_CC_ALL	endoplasmic reticulum	4	1.9E-2	1.4E-1
GOTERM_CC_ALL	cytoplasmic membrane-bounded vesicle	3	4.5E-2	2.8E-1
GOTERM_CC_ALL	membrane-bounded vesicle	3	4.7E-2	2.8E-1
GOTERM_CC_ALL	cytoplasmic vesicle	3	5.9E-2	2.9E-1
GOTERM_CC_ALL	vesicle	3	6.4E-2	2.9E-1
GOTERM_CC_ALL	intracellular organelle part	5	2.6E-1	7.1E-1
GOTERM_CC_ALL	organelle part	5	2.7E-1	6.9E-1
GOTERM_CC_ALL	intracellular organelle lumen	3	3.1E-1	7.2E-1
GOTERM_CC_ALL	organelle lumen	3	3.2E-1	7.2E-1
GOTERM_CC_ALL	membrane-enclosed lumen	3	3.3E-1	7.2E-1
Annotation Cluster 4	**Enrichment Score: 1**	**Count**	**P_Value**	**Benjamini**
GOTERM_MF_ALL	endopeptidase activity	3	2.4E-2	8.7E-1
GOTERM_MF_ALL	peptidase activity, acting on L-amino acid peptides	3	4.9E-2	8.8E-1
GOTERM_MF_ALL	peptidase activity	3	5.3E-2	7.8E-1
GOTERM_MF_ALL	hydrolase activity	4	1.8E-1	9.7E-1
SP_PIR_KEYWORDS	hydrolase	3	1.9E-1	5.3E-1
GOTERM_MF_ALL	catalytic activity	5	4.7E-1	1.0E0
Annotation Cluster 5	**Enrichment Score: 0.85**	**Count**	**P_Value**	**Benjamini**
GOTERM_CC_ALL	extracellular space	3	6.6E-2	2.8E-1
UP_SEQ_FEATURE	disulfide bond	4	1.7E-1	9.1E-1
GOTERM_MF_ALL	hydrolase activity	4	1.8E-1	9.7E-1
SP_PIR_KEYWORDS	disulfide bond	4	1.9E-1	5.3E-1
Annotation Cluster 6	**Enrichment Score: 0.49**	**Count**	**P_Value**	**Benjamini**
GOTERM_CC_ALL	cytoplasmic part	7	5.3E-2	2.8E-1
GOTERM_CC_ALL	organelle membrane	3	1.5E-1	5.0E-1
GOTERM_CC_ALL	intracellular organelle part	5	2.6E-1	7.1E-1
GOTERM_CC_ALL	organelle part	5	2.7E-1	6.9E-1

GOTERM_CC_ALL	cytoplasm	7	2.8E-1	7.0E-1
GOTERM_CC_ALL	intracellular membrane-bounded organelle	7	3.8E-1	7.7E-1
GOTERM_CC_ALL	membrane-bounded organelle	7	3.8E-1	7.6E-1
GOTERM_CC_ALL	intracellular organelle	7	5.4E-1	8.8E-1
GOTERM_CC_ALL	organelle	7	5.4E-1	8.7E-1
GOTERM_CC_ALL	intracellular part	7	7.9E-1	9.8E-1
GOTERM_CC_ALL	intracellular	7	8.3E-1	9.9E-1
Annotation Cluster 7	**Enrichment Score: 0.36**	**Count**	**P_Value**	**Benjamini**
GOTERM_MF_ALL	calcium ion binding	3	1.2E-1	9.3E-1
GOTERM_MF_ALL	cation binding	4	5.5E-1	1.0E0
SP_PIR_KEYWORDS	phosphoprotein	5	5.6E-1	9.3E-1
GOTERM_MF_ALL	ion binding	4	5.6E-1	1.0E0
GOTERM_MF_ALL	metal ion binding	3	8.0E-1	1.0E0
Annotation Cluster 8	**Enrichment Score: 0.24**	**Count**	**P_Value**	**Benjamini**
GOTERM_CC_ALL	intracellular organelle part	5	2.6E-1	7.1E-1
GOTERM_CC_ALL	organelle part	5	2.7E-1	6.9E-1
GOTERM_BP_ALL	regulation of cellular process	3	9.6E-1	1.0E0
GOTERM_BP_ALL	regulation of biological process	3	9.7E-1	1.0E0
GOTERM_BP_ALL	biological regulation	3	9.8E-1	1.0E0
Annotation Cluster 9	**Enrichment Score: 0.05**	**Count**	**P_Value**	**Benjamini**
GOTERM_CC_ALL	membrane part	4	8.5E-1	9.9E-1
GOTERM_CC_ALL	integral to membrane	3	9.0E-1	9.9E-1
GOTERM_CC_ALL	intrinsic to membrane	3	9.1E-1	9.9E-1
Annotation Cluster 10	**Enrichment Score: 0.04**	**Count**	**P_Value**	**Benjamini**
GOTERM_BP_ALL	macromolecule metabolic process	3	9.0E-1	1.0E0
GOTERM_BP_ALL	metabolic process	4	9.0E-1	1.0E0
GOTERM_BP_ALL	primary metabolic process	3	9.6E-1	1.0E0